Quantum entanglement of excitons in coupled quantum dots

Ping Zhang,[1] C. K. Chan,[2] Qi-Kun Xue,[1] and Xian-Geng Zhao[3]
[1]*International Center for Quantum Structure and State Key Laboratory for Surface Physics, Institute of Physics, The Chinese Academy of Sciences, Beijing 100080, China*
[2]*Department of Applied Mathematics, The Hong Kong Polytechnic University, Hong Kong, China*
[3]*Institute of Applied Physics and Computational Mathematics, P.O. Box 8009, Beijing 100088, China*
(Received 19 September 2002; published 22 January 2003)

Optically controlled exciton dynamics in coupled quantum dots is studied. We show that the maximally entangled Bell states and Greenberger-Horne-Zeilinger (GHZ) states can be robustly generated by manipulating the system parameters to be at the avoided crossings in the eigenenergy spectrum. The analysis of population transfer is systematically carried out by using a dressed-state picture. In addition to the quantum dot configuration that has been discussed by Quiroga and Johnson [Phys. Rev. Lett. **83**, 2270 (1999)], we show that the GHZ states also may be produced in a ray of three quantum dots with a shorter generation time.

DOI: 10.1103/PhysRevA.67.012312 PACS number(s): 03.67.Lx, 71.10.Li, 73.61.−r

I. INTRODUCTION

Entanglement is of great interest in many areas of active research in contemporary quantum physics, such as quantum computation [1], quantum teleportation [2], and fundamental tests of quantum mechanics [3,4]. How to design and realize quantum entanglement is extremely challenging due to the intrinsic decoherence, which is caused by the uncontrollable coupling with environmental degrees of freedom. A variety of physical systems have to be chosen to investigate the controlled, entangled states. Among these are trapped ions [5], spins in nuclear magnetic resonance [6], cavity-quantum-electrodynamics systems [7], Josephson junctions [8], and quantum dots [9].

Recently, the combination of progresses in ultrafast opto-electronics [10] and in nanostructure fabrication [11] brings out dense study of the coherent-carrier control in semiconductor quantum dots (QDs). Present ultrafast laser technology allows the coherent manipulation of carrier (electron and/or hole) wave functions on a time scale shorter than typical dephasing times [12]. It has been envisioned that optical excitations in QDs could be successfully exploited for quantum information processing: Quiroga and Johnson [13], and Reina *et al*. [14,15] suggested that the resonant transfer interaction between spatially separated excitons in quantum dots can be exploited to produce many-particle entanglement. Based on numerical analysis of realistic double QDs, Biolatti *et al*. [16], and Troiani *et al.* [17] proposed an *all optical* implementation of quantum information processing. Chen *et al.* [18], and Piermarocchi *et al.* [19] suggested the controlling of spin dynamics of two interacting excitons with pulses of spin-polarized optical excitations. Stievater *et al.* [20] successfully observed the single-qubit rotation of excitonic Rabi oscillation and in a QD. Chen *et al.* [21] measured the quantum entanglement between a pair of electron and hole. Furthermore, Bayer *et al.* [22] demonstrated the entanglement of electron-hole pairs. Up to now, the basic ingredient double-qubit operation, i.e., the controlled-NOT (CNOT) operation has not been experimentally demonstrated.

In this paper, we study the optical control of the exciton dynamics in multiple QDs. Following Ref. [13], we assume that the excitonic occupation operator $\hat{n}_l$ for the lth QD has only two eigenvalues $n_l=0$ and $n_l=1$, corresponding to the absence and the presence of a ground-state exciton. Thus, the single-qubit basis consists of $|0\rangle_l$ and $|1\rangle_l$. The whole computational state space is spanned by the basis $|\mathbf{n}\rangle=\otimes_l|n_l\rangle$ $(n_l=0,1)$. We show that the avoided crossing in eigenenergy spectrum enables the robust generation of maximally entangled Bell state of two qubits and GHZ states of three qubits. The entangled state generation time is analytically obtained by adiabatically eliminating the dark multiexciton states.

This paper is organized as follows. Section II contains the theoretical model: in Sec. II A, we present the Hamiltonian of the multiple QDs equidistant from each other, whereas the Hamiltonian of the QDs with a linear arrangement is presented in Sec. II B. The maximally entangled Bell-state generation is showed in Sec. III. In Sec. IV, the maximally entangled GHZ state generation is shown for the three QDs with equal distance. The GHZ state generation process for the QDs with a linear configuration is analyzed in Sec. V. A summary is given in Sec. VI.

II. THEORETICAL MODEL

We consider a system of N identical QDs radiated by classical optical field. Ignoring any constant energy terms, the Hamiltonian describing the formation of single excitons within the individual QDs and their interdot hopping is given by

$$H(t)=\frac{\varepsilon}{2}\sum_{n=1}^{N}(e_n^\dagger e_n-h_n^\dagger h_n)-\frac{1}{2}\sum_{n,n'=1}^{N}V_{nn'}(e_n^\dagger h_{n'}^\dagger e_{n'}h_n^\dagger + h_n e_{n'}^\dagger h_{n'}^\dagger e_n)+\frac{\Omega(t)}{2}e^{-i\omega t}\sum_{n=1}^{N}e_n^\dagger h_n^\dagger + \frac{\Omega^*(t)}{2}e^{i\omega t}\sum_{n=1}^{N}h_n e_n \tag{1}$$

in the rotating wave approximation. Here $e_n^\dagger$ ($h_n^\dagger$) is the electron (hole) creation operator in the nth QD, ε is the QD band gap, while $V_{nn'}$ represents the interdot Coulomb interaction between the nth and n'th QDs, the time dependence of $\Omega(t)$ describes the laser-pulse shape while ω is the optical frequency. As in the atomic case, the condition $\omega \gg |\Omega(t)|$ enables the rotating wave approximation used in $H(t)$ above.

A. Equidistant quantum dots

In the case that the QDs are equidistant from each other, i.e., $N=2$ dots on a line, $N=3$ dots at the vertices of an equilateral triangle, the interdot Coulomb interaction $V_{nn'} = V$ is independent of n and n'. Thus the spatial symmetry of the Hamiltonian (1) enables us to introduce the global angular momentum operators [13]

$$J_x = \frac{1}{2}\sum_{n=1}^{N} (e_n^\dagger h_n^\dagger + h_n e_n), \tag{2a}$$

$$J_y = \frac{-i}{2}\sum_{n=1}^{N} (e_n^\dagger h_n^\dagger - h_n e_n), \tag{2b}$$

$$J_z = \frac{1}{2}\sum_{n=1}^{N} (e_n^\dagger e_n - h_n h_n^\dagger), \tag{2c}$$

which obey standard angular-momentum commutation relationships $[J_\alpha, J_\beta] = iJ_\gamma$, where (α,β,γ) represent a cyclic permutation of (x,y,z). In terms of these new operators the Hamiltonian for the equidistant QDs can be rewritten as a direct sum over various J-invariant Hamiltonian, i.e.,

$$H(t) = \bigoplus_{J=0}^{N/2} H^{(J)}(t), \tag{3}$$

where

$$H^{(J)}(t) = \varepsilon J_z - V(J^2 - J_z^2) + \frac{1}{2}\Omega(t)e^{-i\omega t}J_+ + \frac{1}{2}\Omega^*(t)e^{-i\omega t}J_-, \tag{4}$$

where $J_\pm = J_x \pm iJ_y$ are the usual raising and lowering operators. To proceed we introduce the time dependent unitary transformation $U = \exp(-i\omega t J_z)$. The transformed Hamiltonian in the rotating frame is

$$H_{RF}^{(J)} = \Delta J_z - V(J^2 - J_z^2) + \Omega_x(t)J_x + \Omega_y(t)J_y, \tag{5}$$

where Δ is the detuning from resonant excitation, $\Omega_x(t) = \mathrm{Re}[\Omega(t)]$ and $\Omega_y(t) = \mathrm{Im}[\Omega(t)]$ are the Rabi coupling strength along the x and y axes, respectively.

B. Quantum dots with a linear configuration

When the quantum dots are prepared along a ray, the value of $V_{n,n'}$ depends on n or n'. Here, we assume that the exciton transfer can only be excited by the hopping between the nearest neighbors. Thus, only $V_{n,n+1} = V$ $(n = 1,2,\ldots,N-1)$ is not zero, while the other $V_{nn'}$ are zero in the tight-binding approximation. In this case, we introduce the local 1/2-pseudospin operators

$$\sigma_n^x = \frac{1}{2}(e_n^\dagger h_n^\dagger + h_n e_n), \tag{6a}$$

$$\sigma_n^y = \frac{-i}{2}(e_n^\dagger h_n^\dagger - h_n e_n), \tag{6b}$$

$$\sigma_n^z = \frac{1}{2}(e_n^\dagger e_n - h_n h_n^\dagger), \tag{6c}$$

which obey the commutation relationships among three Pauli matrices $[\sigma_n^\alpha, \sigma_{n'}^\beta] = i\delta_{n,n'}\sigma_n^\gamma$. The Hamiltonian can be rewritten in terms of these local 1/2-spin operators as

$$H(t) = \varepsilon \sum_n^N \sigma_n^z - V\sum_{n=1}^{N-1} (\sigma_n^- \sigma_{n+1}^+ + \sigma_n^+ \sigma_{n+1}^-) + \frac{1}{2}\Omega(t)e^{-i\omega t}\sum_{n=1}^{N} \sigma_n^+ + \frac{1}{2}\Omega^*(t)e^{i\omega t}\sum_{n=1}^{N} \sigma_n^-, \tag{7}$$

where $\sigma_n^\pm = \sigma_n^x \pm i\sigma_n^y$. In deriving Eq. (7), we have neglected all constant energy terms that have no contribution to the dynamics. Again, we transform the Hamiltonian (7) into the rotating frame by introducing the unitary transformation $U = \exp(-i\omega_{las} t \Sigma_n^N \sigma_n^z)$ as follows:

$$H_{RF} = \sum_n^N \Delta\sigma_n^z - V\sum_{n=1}^{N-1} (\sigma_n^- \sigma_{n+1}^+ + \sigma_n^+ \sigma_{n+1}^-) + \Omega(t)\sum_{n=1}^{N} \sigma_n^+ + \Omega^*(t)\sum_{n=1}^{N} \sigma_n^-. \tag{8}$$

In the absence of optical field, the Hamiltonian (8) is identical to an one-dimensional X-Y model in the magnetic system. In the limit $N\to\infty$, one can obtain the exact ground state with the help of the well-known Jordan-Wigner transformation.

III. BELL-STATE GENERATION IN DOUBLE QDS

To give a systematic analysis on the exciton dynamics, we start with the exploitation of the maximally entangled Bell-state generation. In the absence of optical excitation, there is no interband transition, so there are no excitons in the double QDs, i.e., we start with the vacuum state $|00\rangle$. In the following we will show how to generate the maximally entangled Bell state of the form $|\Psi_{Bell}\rangle = (1/\sqrt{2})(|00\rangle + e^{i\phi}|11\rangle)$ with 0 (1) denoting a zero-exciton (single-exciton) QD. According to Eq. (2), the initial vacuum state $|00\rangle$ is identical to $|J=1, J_z=-1\rangle$ (denoted by $|1,-1\rangle$ in the following) in the angular-momentum representation, thus the subsequent time evolution in the presence of the laser field will be restricted to the $J=1$ subspace. This means that the antisymmetric single-exciton state is light inactive. The evolution of any initial state $|\Psi(0)\rangle$ under the action of $H_{RF}^{(J=1)}$ in Eq. (5) can be thus expressed as $|\Psi(t)\rangle = c_1(t)|1,1\rangle + c_2(t)|1,0\rangle + c_3(t)|1,-1\rangle$ in the angular-momentum representation. Here, the coefficients $c_k(t)$ are determined by the Schrödinger equation

$$i\begin{pmatrix}\dot{c}_1\\ \dot{c}_2\\ \dot{c}_3\end{pmatrix} = \begin{pmatrix}\Delta - V & |\Omega|e^{-i\varphi}/\sqrt{2} & 0\\ |\Omega|e^{i\varphi}/\sqrt{2} & -2V & |\Omega|e^{-i\varphi}/\sqrt{2}\\ 0 & |\Omega|e^{i\varphi}/\sqrt{2} & -\Delta - V\end{pmatrix}\begin{pmatrix}c_1\\ c_2\\ c_3\end{pmatrix}, \tag{9}$$

where $|\Omega| = \sqrt{\Omega_x^2+\Omega_y^2}/2$ and $\varphi = \tan^{-1}(\Omega_y/\Omega_x)$. Therefore, the probability ρ_{Bell} for finding the maximally entangled Bell state in a double quantum dot is given by

$$\rho_{Bell} = \frac{1}{2}|c_3(t) + e^{i\phi}c_1(t)|^2. \tag{10}$$

The eigenenergies associated with the Schrödinger equation (9) can be solved analytically for general values of driving frequency ω. For brevity, we do not give the explicit expressions here. Instead, we illustrate in Fig. 1 the spectrum features by plotting the eigenenergies as a function of driving frequency. It shows in Fig. 1 that an avoided crossing between energies E_1 and E_2 occurs at the value of $\omega=\varepsilon$, which corresponds to the exact resonance condition $\Delta=0$. The occurrence of avoided crossing in the energy spectrum implies the strong resonant oscillation between the corresponding eigenstates. The oscillation frequency can be easily read out from the difference between the energy levels at $\Delta=0$. In this case, the eigenenergies and eigenstates (not normalized) of Eq. (9) are

$$|\varphi_1\rangle = |1,1\rangle - \frac{b}{\sqrt{2}|\Omega|}|1,0\rangle + |1,-1\rangle, \quad E_1 = a - V, \tag{11a}$$

$$|\varphi_2\rangle = -|1,1\rangle + |1,-1\rangle, \quad E_2 = -2V, \tag{11b}$$

$$|\varphi_3\rangle = |1,1\rangle - \frac{a}{\sqrt{2}|\Omega|}|1,0\rangle + |1,-1\rangle, \quad E_3 = b - V, \tag{11c}$$

where $a = (-V - \sqrt{V^2+4|\Omega|^2})/2$, and $b = (-V + \sqrt{V^2+4|\Omega|^2})/2$. From Eq. (11), we can see that for a weak driving field $|\Omega| \ll V$, the states $|\varphi_1\rangle$ and $|\varphi_2\rangle$ are nearly degenerate and dominated by the zero-exciton state $|1,-1\rangle$ and double-exciton state $|1,1\rangle$, whereas the state $|\varphi_3\rangle$ is dominated by the single-exciton state $|1,0\rangle$. Starting from the initial state $|1,-1\rangle$, we expect its resonant oscillation with $|1,1\rangle$, with the oscillation frequency approximated by

$$\omega_r = E_2 - E_1 \simeq |\Omega|^2/V. \tag{12}$$

Because the population of the single-exciton state remains very small during time evolution, we can approximate $c_2(t)$ in Eq. (9) to first order of $|\Omega|/V$

$$c_2(t) = \frac{|\Omega|}{\sqrt{2}V}e^{i\varphi}c_1(t) + \frac{|\Omega|}{\sqrt{2}V}e^{-i\varphi}c_3(t). \tag{13}$$

By introducing $c_2(t)$ from Eq. (13) in the Schrödinger equation we reduce the system to an effective two-level system. The reduced equation has the form

$$i\begin{pmatrix}\dot{c}_1\\ \dot{c}_3\end{pmatrix} = \begin{pmatrix}-V + \dfrac{|\Omega|^2}{2V} & \dfrac{|\Omega|^2}{2V}e^{-i2\varphi}\\ \dfrac{|\Omega|^2}{2V}e^{i2\varphi} & -V + \dfrac{|\Omega|^2}{2V}\end{pmatrix}\begin{pmatrix}c_1(t)\\ c_3(t)\end{pmatrix}. \tag{14}$$

Thus, with the initial zero-exciton state, we have the time evolution of the system as follows:

$$c_1(t) = -i\exp\left[i\left(V + \frac{|\Omega|^2}{2V}\right)t\right]\exp(-i2\varphi)\sin[|\Omega|^2 t/(2V)], \tag{15a}$$

$$c_3(t) = \exp\left[i\left(V + \frac{|\Omega|^2}{2V}\right)t\right]\cos[|\Omega|^2 t/(2V)]. \tag{15b}$$

Substituting Eq. (15) into Eq. (10), we have the probability for finding the Bell state $(1/\sqrt{2})(|00\rangle + e^{i\phi}|11\rangle)$ at time t,

$$\rho_{Bell}(t) = \frac{1}{2}[1 + \sin(\omega_r t)\cos(\phi - 2\varphi - \pi/2)], \tag{16}$$

where $\omega_r = |\Omega|^2/V$. From Eq. (16), one can see that the Bell state with an arbitrary phase can be generated by controlling the Rabi coupling strength. In the case of $\Omega_y=0$ and constant value of Ω_x, we obtain the same result as in Ref. [13]. Note that the Bell-state generation time is significantly shortened by applying stronger laser pulses. This is important because a short pulse length for Bell-state generation is fundamental to experimental observation of such maximally entangled state that is impeded by inevitable decoherence occurred in the realistic double quantum dot system. We find Eq. (16) is remarkably valid for the slowly varying amplitude $\Omega(t)$.

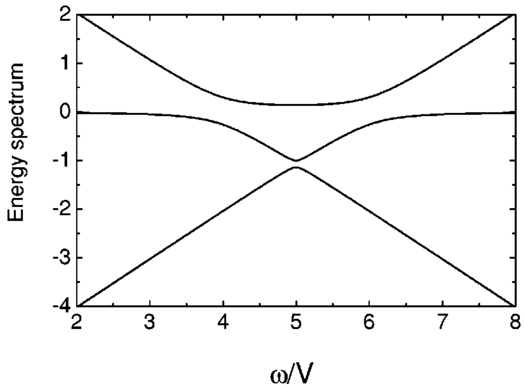

FIG. 1. The energy spectrum of a double quantum dot system as a function of the frequency of laser pulse. Parameters are $\varepsilon=5V$ and $|\Omega|=0.2V$.

For numerical calculations, we consider Gaussian temporal pulse shape for the excitation laser. The time-dependent Schrödinger equation is numerically integrated using the fourth-order Runge-Kutta scheme. The results of the Bell-state generation dynamics are shown in Fig. 2. The laser-pulse shape is plotted as a dotted line. The square amplitudes of the vacuum state $|00\rangle$ and biexciton state $|11\rangle$ are denoted by $|c_3|^2$ and $|c_1|^2$, respectively, and plotted as solid lines. The population of single-exciton state is given by $|c_2|^2$. As one can see from Fig. 2, the quantity of $|c_2|^2$ is always near zero during time evolution. This light-inactive property enables us to adiabatically eliminate its contribution and reduce the system to an effective two-level model, as we have done in deriving Eq. (16). The probability ρ_{Bell} for finding the maximally entangled Bell state $(1/\sqrt{2})(|00\rangle+e^{i\pi/2}|11\rangle)$ is also shown in the figure as dashed line. It achieves its maximum value of almost unity in the middle of optical excitation and remains unchanged afterwards.

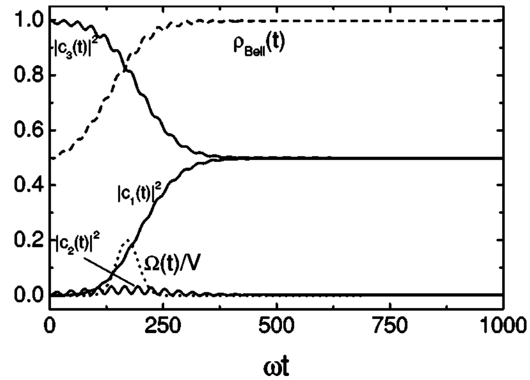

FIG. 2. The Bell-state generation process as a function of time. The pulse shape $\Omega(t)$ is plotted as a dotted line. The probability $\rho_{Bell}(t)$ of maximally entangled Bell state is shown as a dashed line. The population of three exciton number states are also plotted (solid lines).

IV. GHZ STATE GENERATION IN EQUIDISTANT QUANTUM DOTS

In this section, we show the optical excitation of maximally entangled GHZ state $(1/\sqrt{2})(|000\rangle+e^{i\phi}|111\rangle)$ in three coupled QDs equidistant from each other. The initial state is chosen to be the vacuum state $|000\rangle$, i.e., the eigenstate $|3/2,-3/2\rangle$ of the angular-momentum operator J_z. Thus, the subsequent time evolution of the system is confined to the $J=3/2$ subspace. The evolution of wave function can be expressed as

$$|\Psi(t)\rangle=c_1(t)|3/2,3/2\rangle+c_2(t)|3/2,1/2\rangle+c_3(t)|3/2,-1/2\rangle+c_4(t)|3/2,-3/2\rangle,$$

where the coefficients $c_k(t)$ are determined by the Schrödinger equation

$$i\frac{d}{dt}\begin{pmatrix}c_1\\c_2\\c_3\\c_4\end{pmatrix}=\begin{pmatrix}\frac{3(-V+\Delta)}{2} & \sqrt{3}|\Omega|e^{-i\varphi}/2 & 0 & 0\\ \sqrt{3}|\Omega|e^{i\varphi}/2 & \frac{-7V+\Delta}{2} & |\Omega|e^{-i\varphi} & 0\\ 0 & |\Omega|e^{-i\varphi} & \frac{-7V-\Delta}{2} & \sqrt{3}|\Omega|e^{-i\varphi}/2\\ 0 & 0 & \sqrt{3}|\Omega|e^{i\varphi}/2 & \frac{3(-V-\Delta)}{2}\end{pmatrix}\begin{pmatrix}c_1\\c_2\\c_3\\c_4\end{pmatrix}. \tag{17}$$

The probability for finding the maximally entangled GHZ state is given by

$$\rho_{GHZ}=\frac{1}{2}|c_4(t)+e^{i\phi}c_1(t)|^2. \tag{18}$$

Figure 3 shows the eigenenergy spectrum of the Hamiltonian in Eq. (17) as a function of the driving frequency. It shows that there are two avoided crossings in the energy spectrum where the driving frequency approaches to satisfy the resonance condition $\Delta=0$, which implies resonant oscillations between the relevant eigenstates. The oscillation fre-

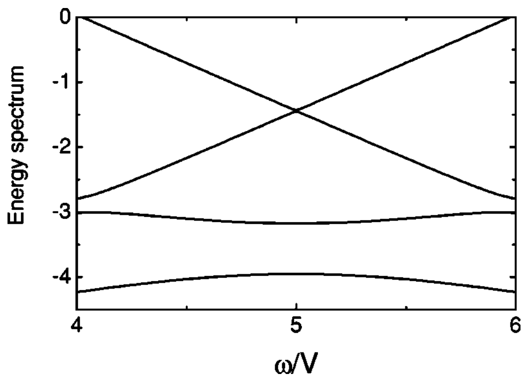

FIG. 3. The energy spectrum of a three quantum dot system as a function of the frequency of laser pulse. Parameters are $\varepsilon=5V$ and $|\Omega|=0.2V$.

quency can be obtained from the difference of the energy levels at $\Delta=0$. In this case, the eigenenergies are

$$E_{1,2}=-5V/2\mp|\Omega|-\sqrt{(-V\mp|\Omega|)^2+3|\Omega|^2}, \quad (19a)$$

$$E_{3,4}=-5V/2\mp|\Omega|+\sqrt{(-V\mp|\Omega|)^2+3|\Omega|^2}. \quad (19b)$$

The corresponding unnormalized eigenstates are given by

$$|\varphi_i\rangle=|3/2,-3/2\rangle+\delta_i|3/2,-1/2\rangle\mp\delta_i|3/2,1/2\rangle +|3/2,3/2\rangle \quad (i=1,\ldots,4), \quad (20)$$

where $\delta_i=(E_i+3V/2)/(\sqrt{3}|\Omega|)$. From Eqs. (19) and (20) one can see that for a weak driving field $|\Omega|\ll V$, the states $|\varphi_3\rangle$ and $|\varphi_4\rangle$ are nearly degenerate and dominated by the vacuum state $|3/2,-3/2\rangle$ and triexciton state $|3/2,3/2\rangle$, whereas the states $|\varphi_1\rangle$ and $|\varphi_2\rangle$ are dominated by the single-exciton state $|3/2,-1/2\rangle$ and biexciton state $|3/2,1/2\rangle$. Thus, under the initial vacuum state condition, the dynamic evolution of the system is characterized by the resonant oscillation between $|3/2,-3/2\rangle$ and $|3/2,3/2\rangle$, whereas the contribution from the states $|3/2,-1/2\rangle$ and $|3/2,1/2\rangle$ can be neglected. To adiabatically eliminate these two states from the dynamics, we introduce the unitary transformation

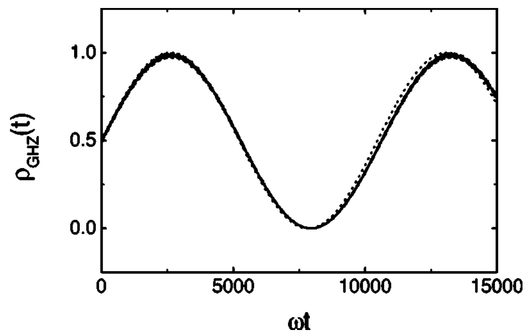

FIG. 4. Exact numerical (solid line) and approximate results of the time evolution of the probability $\rho_{GHZ}(t)$. Parameters are $\Delta=0$, $|\Omega|=0.2V$, and $\varphi=0$.

$$R=\begin{pmatrix} 1 & 0 & 0 & 0 \\ 0 & \frac{1}{\sqrt{2}} & \frac{1}{\sqrt{2}} & 0 \\ 0 & \frac{1}{\sqrt{2}}e^{i\varphi} & -\frac{1}{\sqrt{2}}e^{i\varphi} & 0 \\ 0 & 0 & 0 & 1 \end{pmatrix}, \quad (21)$$

which transforms the state components $c_2(t)$ and $c_3(t)$ into the diagonal representation. Defining the state vector $\vec{c}=(c_1,\ldots,c_4)^T$, supposing $\vec{c}(t)=e^{i3Vt/2}R\vec{d}(t)$, we obtain the equation of motion for the reduced state vector,

$$i\frac{d}{dt}\vec{d}(t)=H_d^{(J=3/2)}\vec{d}(t), \quad (22)$$

where the transformed resonant Hamiltonian $(\Delta=0)$ is

$$H_d^{(J=3/2)}=R^+H_{RF}^{(J=3/2)}R+3V/2=\begin{pmatrix} 0 & \sqrt{\frac{3}{8}}|\Omega|e^{-i\varphi} & \sqrt{\frac{3}{8}}|\Omega|e^{-i\varphi} & 0 \\ \sqrt{\frac{3}{8}}|\Omega|e^{i\varphi} & -2V+|\Omega| & 0 & \sqrt{\frac{3}{8}}|\Omega|e^{-i2\varphi} \\ \sqrt{\frac{3}{8}}|\Omega|e^{i\varphi} & 0 & -2V-|\Omega| & -\sqrt{\frac{3}{8}}|\Omega|e^{-i2\varphi} \\ 0 & -\sqrt{\frac{3}{8}}|\Omega|e^{i2\varphi} & -\sqrt{\frac{3}{8}}|\Omega|e^{i2\varphi} & 0 \end{pmatrix}. \quad (23)$$

The two components d_2 and d_3 can now be adiabatically eliminated in the same matter in deriving Eq. (15). Thus, one obtains the effective two-state approximation as follows:

$$i\frac{d}{dt}d_1(t)=\chi_1 d_1(t)+e^{-i3\varphi}\chi_2 d_4(t), \tag{24a}$$

$$i\frac{d}{dt}d_4(t)=e^{i3\varphi}\chi_2 d_1(t)+\chi_1 d_4(t), \tag{24b}$$

where

$$\chi_1=\frac{3|\Omega|^2}{16V-8|\Omega|}+\frac{3|\Omega|^2}{16V+8|\Omega|}, \tag{25a}$$

$$\chi_2=\frac{3|\Omega|^2}{16V-8|\Omega|}-\frac{3|\Omega|^2}{16V+8|\Omega|}. \tag{25b}$$

With the initial condition $d_1(0)=0$ and $d_4(0)=1$, one obtains the solution of Eq. (24),

$$d_1(t)=-ie^{-i3\varphi}e^{i\chi_1 t}\sin(\chi_2 t), \tag{26a}$$

$$d_4(t)=e^{i\chi_1 t}\cos(\chi_2 t). \tag{26b}$$

Substituting Eqs. (26) into the expression for $\rho_{GHZ}(t)$, one obtains the probability for finding the maximally entangled GHZ state $|\Psi_{GHZ}\rangle$,

$$\rho_{GHZ}(t)=\frac{1}{2}[1+\sin(\omega_r t)\cos(\phi-3\varphi-\pi/2)], \tag{27}$$

where the oscillating frequency $\omega_r=2\chi_2\simeq 3|\Omega|^3/(8V^2)$. Equation (27) shows that the maximally entangled GHZ state with an arbitrary phase can be generated by a selective pulse of the laser field. In particular, in the case of $\Omega_y=0$, a $\pi/2$ pulse produces the GHZ state $(|000\rangle+e^{i\pi/2}|111\rangle)/\sqrt{2}$ at time $\tau_G=4\pi V^2/(3|\Omega|^3)$. Note that the result of Eq. (27) in the case of $\varphi=0$ was first obtained by Quiroga and Johnson in the density-matrix formalism [13]. Our approach, which is based on a combination of eigenenergy spectrum analysis and adiabatic elimination of dark states, may be combined with the density-matrix method to highlight the physical prospects in preparing entangled qubits.

To compare the analytical and numerical solutions for the unitary evolution described above. We show in Fig. 4 the time evolution of $\rho_{GHZ}(t)$ with $\Omega_y=0$ and a constant value of $\Omega_x=0.2V$. The solid line in Fig. 4 is the exact solution obtained by numerically integrating Schrödinger equation (17), whereas the dotted line is the result of Eq. (27). Clearly our two-state approximation describes the system's evolution very well when compared with the exact numerical solution, implying that the system's quantum state at time τ_G corresponds to a maximally entangled GHZ state $|\Psi_{GHZ}\rangle=(|000\rangle+e^{i\pi/2}|111\rangle)/\sqrt{2}$. For a more realistic consideration, we employ Gaussian temporal pulse shape and present in Fig. 5 the generation process of the GHZ state $|\Psi_{GHZ}\rangle$. Again, one can see that the dynamics of the system is dominated by the entanglement of the vacuum state and triexciton state, while the population of single-exciton and biexciton states are strongly suppressed. As a consequence, the probability ρ_{GHZ} achieves and remains unity after laser pulse.

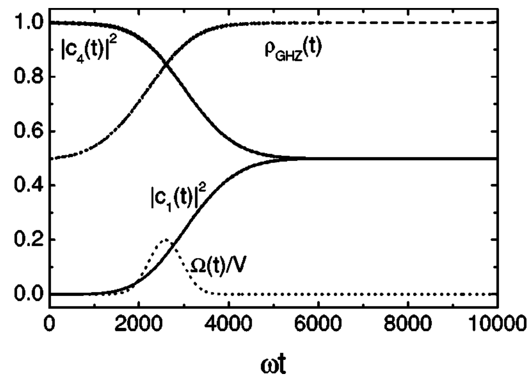

FIG. 5. The GHZ state generation process. The pulse shape $\Omega(t)$ is plotted as a dotted line. The populations of single-exciton and biexciton states are again strongly suppressed and the probability $\rho_{GHZ}(t)$ (dashed line) is unity after laser pulse.

V. GHZ STATE GENERATION IN A RAY OF THREE COUPLED QDS

In this section, we show the optical excitation of maximally entangled GHZ states in a ray of three coupled QDs. The dynamics of the system is now described by the Hamiltonian (8). In an exciton number basis consisting of $|000\rangle$, $|100\rangle$, $|010\rangle$, $|001\rangle$, $|110\rangle$, $|011\rangle$, $|101\rangle$, and $|111\rangle$, the Schrödinger equation is

$$i\frac{d}{dt}\begin{pmatrix} c_1\\ c_2\\ c_3\\ c_4\\ c_5\\ c_6\\ c_7\\ c_8\end{pmatrix}=\begin{pmatrix} -3\Delta & \Omega^* & \Omega^* & \Omega^* & 0 & 0 & 0 & 0\\ \Omega & -\Delta & -V & 0 & \Omega^* & 0 & \Omega^* & 0\\ \Omega & -V & -\Delta & -V & \Omega^* & \Omega^* & 0 & 0\\ \Omega & 0 & -V & -\Delta & 0 & \Omega^* & \Omega^* & 0\\ 0 & \Omega & \Omega & 0 & \Delta & 0 & -V & \Omega^*\\ 0 & 0 & \Omega & \Omega & 0 & \Delta & -V & \Omega^*\\ 0 & \Omega & 0 & \Omega & -V & -V & \Delta & \Omega^*\\ 0 & 0 & 0 & 0 & \Omega & \Omega & \Omega & 3\Delta \end{pmatrix}\begin{pmatrix} c_1\\ c_2\\ c_3\\ c_4\\ c_5\\ c_6\\ c_7\\ c_8\end{pmatrix}. \tag{28}$$

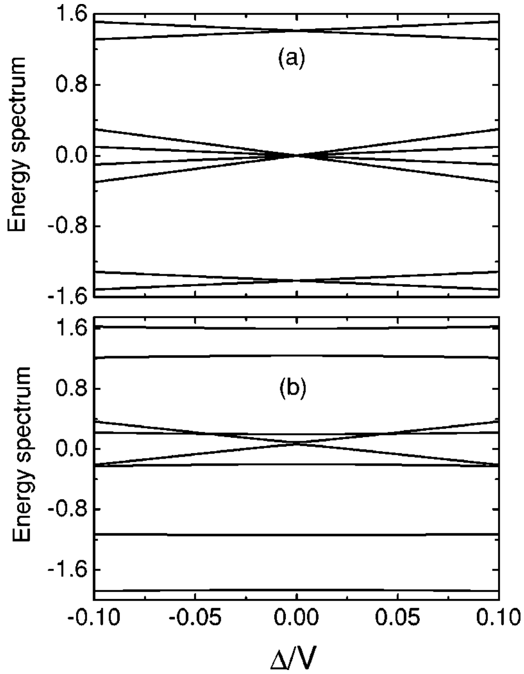

FIG. 6. The energy spectrum of a ray of three quantum dots as a function of detuning Δ (a) in the absence of laser field, (b) in the presence of laser field for the value of $|\Omega|=0.2V$. Other parameters are $\varepsilon=5V$.

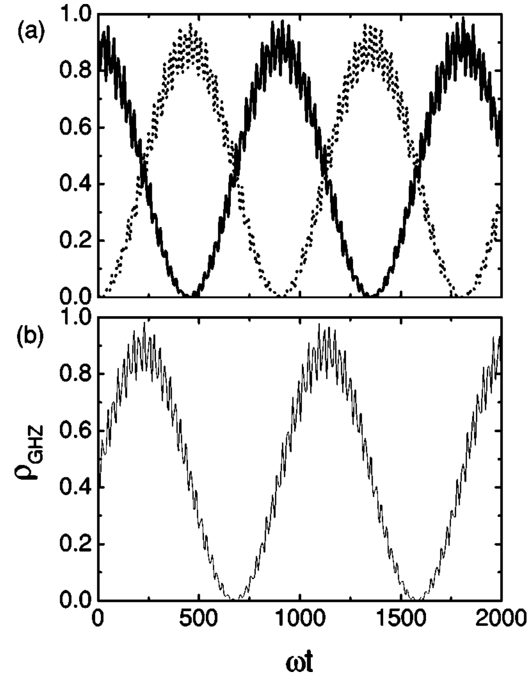

FIG. 7. (a) Time evolution of the population of the vacuum state (solid line) and triexciton state (dotted line). (b) Time evolution of the probability $\rho_{GHZ}(t)$ for finding the maximally entangled GHZ state ($\phi=\pi/2$) in a ray of three coupled quantum dots. Parameters are $\Delta=0$, $\varepsilon=5V$, $|\Omega|=0.2V$, and $\varphi=0$.

The probability for finding the GHZ state $|\Psi_{GHZ}\rangle=(|000\rangle+e^{i\phi}|111\rangle)/\sqrt{2}$ is given by $\rho_{GHZ}(t)=|c_8(t)+e^{i\phi}c_1|^2/2$.

Without knowing an analytical approximation of Eq. (28), we turn to numerically show the optical excitation of the GHZ state. In the absence of laser field, one can see from Eq. (28) that the subspaces of vacuum, exciton, biexciton, and triexciton states are not coupled. In this case, the typical energy spectrum is shown in Fig. 6(a) as a function of detuning Δ. It shows in Fig. 6(a) that when Δ approaches to zero, the spectrum is characterized by three degenerate energies. The degenerate states with energy $E=0$ consist of vacuum state $|000\rangle$, triexciton state $|111\rangle$, and a pair of single-exciton and biexciton states. The other two set of degenerate states consist of a pair of single- and double-exciton states, respectively. The energy spectrum features are greatly changed in the presence of the optical field, which can be seen from Fig. 6(b). It reveals that the degeneracies are completely broken and three avoided crossings develop near $\Delta=0$. Among these crossings, the energy splitting between the eigenstates dominated by the states $|000\rangle$ and $|111\rangle$ is smallest, since these two states are coupled in an indirect way. Therefore, starting from the state $|000\rangle$, we expect that the subsequent time evolution of the system is featured by the resonant oscillations between the vacuum and triexciton states. This is numerically verified in Fig. 7, where Fig. 7(a) plots the probabilities for finding the system in the zero- and triple-exciton states and Fig. 7(b) the probability $\rho_{GHZ}(t)$. Clearly it shows that a selective pulse of laser field can be used to produce the maximally entangled GHZ states in a ray of three QDs. Note that compared with the results in Fig. 4, it shows in Fig. 7 that *the GHZ state generation time for a linear configuration is shorter than for a equidistant configuration*. Thus, the linear configuration of three QDs is preferred to implement the maximally entangled GHZ states for its shorter generation time.

VI. CONCLUSION

In summary, we have studied the optically controlled exciton dynamics in multiple QD systems. We have shown that the robust occurrence of avoided crossing in the eigenenergy spectrum enables the dynamics to be confined to a reduced two-state Hilbert space, in which the generation of maximally entangled Bell states and GHZ states with an arbitrary phase can be controlled by selective pulses of classical coherent optical light. The entangled state generation time decreases significantly with an increase of the laser-pulses strength. We have also found that the GHZ states can be implemented in a three-QD system with a linear configuration, with the generation time much shorter than in an equidistant configuration. The results are expected to be useful in exploiting the realizations of entanglement in quantum dot systems.

ACKNOWLEDGMENTS

This work was partially supported by a grant from the Research Committee of The Hong Kong Polytechnic University (Grant No. G-T308), by NSF (Grant Nos. 60021403 and 10274007), and by MOST of China (Grant No. G001CB3095).

[1] A. Ekert and R. Jozsa, Rev. Mod. Phys. **68**, 733 (1996).
[2] C.H. Bennett, G. Brassard, C. Crepeau, R. Jozsa, A. Peres, and W.K. Wootters, Phys. Rev. Lett. **70**, 1895 (1993).
[3] J.S. Bell, Physics (Long Island City, N.Y.) **1**, 195 (1965).
[4] D.M. Greenberger, M.A. Horne, and A. Zeilinger, Am. J. Phys. **58**, 1131 (1990).
[5] J.I. Cirac and P. Zoller, Phys. Rev. Lett. **74**, 4091 (1995).
[6] N.A. Gershenfeld and I.L. Chuang, Science **275**, 350 (1997).
[7] P. Domokos *et al.*, Phys. Rev. A **52**, 3554 (1995).
[8] Y. Makhlin, G. Schön, and A. Shnirman, Nature (London) **398**, 305 (1999).
[9] D. Loss and D.P. DiVincenzo, Phys. Rev. A **57**, 120 (1998).
[10] J. Shah, *Ultrafast Spectroscopy of Semiconductors and Semiconductor Nanostructures* (Springer, Berlin, 1996).
[11] L. Jacak, P. Hawrylak, and A. Wojs, *Quantum Dots* (Springer, Berlin, 1998).
[12] N.H. Bonadeo *et al.*, Science **282**, 1473 (1998).
[13] L. Quiroga and N.F. Johnson, Phys. Rev. Lett. **83**, 2270 (1999).
[14] J.H. Reina, L. Quiroga, and N.F. Johnson, Phys. Rev. A **62**, 012305 (2000).
[15] J.H. Reina, L. Quiroga, and N.F. Johnson, e-print quant-ph/0009035.
[16] E. Biolatti, R.C. Iotti, P. Zanardi, and F. Rossi, Phys. Rev. Lett. **85**, 5647 (2000).
[17] F. Troiani, U. Hohenester, and E. Molinari, Phys. Rev. B **62**, R2263 (2000).
[18] P. Chen, C. Piermarocchi, and L.J. Sham, e-print cond-mat/0102482.
[19] C. Piermarocchi, P. Chen, Y.S. Dale, and L.J. Sham, e-print cond-mat/0102482.
[20] T.H. Stievater *et al.*, Phys. Rev. Lett. **87**, 133603 (2001).
[21] G. Chen *et al.*, Science **289**, 1906 (2000).
[22] M. Bayer *et al.*, Science **291**, 451 (2001).